Rodriguez Cortina, J.; Clemente Polo, G.; Sanjuán Pellicer, MN.; Bon Corbín, J. (2014). Modeling drying kinetics of thyme (thymus vulgaris l.): theoretical and empirical models, and neural networks. Food Science and Technology International. 20(1):13-22. doi:10.1177/1082013212469614.

MODELING DRYING KINETICS OF THYME (*THYMUS VULGARIS* L.): THEORETICAL AND EMPIRICAL MODELS, AND NEURAL NETWORKS

J. Rodríguez, G. Clemente, N. Sanjuán, J. Bon

ASPA Group, Food Technology Department, Polytechnic University of Valencia, Cno de Vera s/n, 46071, Valencia, Spain; tel.+34 963879133, e-mail: jbon@tal.upv.es

Abstract

The drying kinetics of thyme was analyzed by considering different conditions: air temperature of between 40-70º C, and air velocity of 1 m/s. A theoretical diffusion model and eight different empirical models were fitted to the experimental data. From the theoretical model application the effective diffusivity per unit area of the thyme was estimated (between $3.68\ 10^{-5}$ and $2.12\ 10^{-4}$ s^{-1}). The temperature dependence of the effective diffusivity was described by the Arrhenius relationship with activation energy of 49.42 kJ/mol. Eight different empirical models were fitted to the experimental data. Additionally, the dependence of the parameters of each model on the drying temperature was determined, obtaining equations that allow estimating the evolution of the moisture content at any temperature in the established range. Furthermore, artificial neural networks (ANNs) were developed and compared with the theoretical and empirical models using the percentage of the relative errors (ER) and the explained variance (VAR). The ANNs were found to be more accurate predictors of moisture evolution with VAR $\geq$ 99.3% and ER $\leq$ 8.7%.

Keywords: mathematical models, fitting models, model comparisons.

1. Introduction

The food industry is becoming increasingly interested in aromatic herbs, mainly of the Lamiaceae family, for its medicinal properties and for possessing a wide variety of antioxidant components such as phenolic compounds. Thyme (*Thymus vulgaris* L.) is a member of the Lamiaceae family, native to Mediterranean countries. It is very important for the horticultural industry and can be used in herbal teas or as a condiment and the essential oils extracted from its fresh leaves and flowers are known for their different beneficial properties: antiseptic, carminative, antimicrobial and antioxidative (Shati and Elsaid, 2009). However, thyme is perishable, which requires the use of preservation methods in order to lengthen its useful life for further use (Doymaz, 2009).

Hot air drying is one of the oldest food preservation processes. However, the exposure to thermal energy can affect important food properties, such as the chemical composition, texture, color and flavor. Therefore, the selection of a suitable drying method, developing an appropriate mathematical model, and the determination of the optimum operating parameters, are essential to achieve high quality, minimum cost products with a maximum yield (Clemente et al., 2010).

Many mathematical models have been proposed to describe the drying process. These models can be categorized as theoretical, semi theoretical and empirical (Ozdemir and Devres, 1999; McMinn, 2006). A great deal of research has been carried out into the mathematical modeling and experimental drying processes of different agro-based products, such as kiwifruits (Maskan, 2001), red pepper (Akpinar et al., 2003), aromatic plants (Akpinar, 2006), tea leaves (Ghodake et al., 2006), rosemary leaves (Arslan and Ozcan, 2008), onion (Lee and Kim, 2008), and spinach leaves (Doymaz, 2009).

Food processing is a complex system due to the complicated interactions that take place between various components. This makes it more difficult to develop

mathematical models, since, in principle, it is necessary to understand the major mechanisms involved in the process. Despite the criticism that it is not based on fundamental and/or individuals laws, an artificial neural network is an effective tool for developing mathematical models of relatively complex processes, mainly due to its ability to learn (Zhou and Therdthai, 2010). ANNs are being applied in agri-food processes including drying, baking, osmotic dehydration and high-pressure processes as well as in the estimation of food properties and quality indicators (Sablani and Rahman, 2003; Chegini, 2008). Recently, modeling the drying of food products using ANNs has gained momentum for irregular geometries (Erenturk and Erenturk, 2007); however, there is no reference in literature to the modeling of thyme drying using ANNs.

The objectives of this study were to apply and compare a theoretical model, different empirical models, and ANNs to predict the evolution of thyme moisture content during the convective drying at different temperatures.

2. Materials and methods

2.1. Sample preparation

Fresh thyme samples (*Thymus vulgaris* L.) were acquired from a grower/producer in Valencia, Spain, and kept in refrigeration (4 ºC) for their later use. The initial moisture content was determined according to the AOAC standards (1997), obtaining the following results: 78.42 % (w.b.) ± 3.26.

2.2. Drying experiments

Several drying experiments were carried out in triplicate, at constant temperatures of 40, 50, 60 and 70 °C, and an air velocity of 1.0 m/s; the relative humidity of the hot air was between 3.7–18 %. In every experiment, the sample's initial weight was 50 g

(±0.5 g), and the drying process was performed until the final moisture content was about 10 % (w.b.). The thyme samples were distributed uniformly into de drying chamber, forming a bed with a thickness of 2.99±0.2 cm, and the air flow passed through the bed.

A completely automatic, laboratory scale convective drier (Sanjuán, et al., 2003), with control of air temperature and velocity was used (Figure 1). The drying chamber was formed by a cylindrical sample holder which was periodically weighed (at 5 min intervals), and the weight was measured and registered using a balance connected to a computer.

2.3 Mathematical modeling

2.3.1 Theoretical model

Considering that the product behaves like an infinite slab, a theoretical model (Eqs. 1 to 3) based on Fick's particular law was applied, taking the following simplifications into account: (i) negligible external resistance to mass transfer; (ii) isotropic and homogenous material; (iii) negligible material shrinkage.

$$\frac{W(t) - W_e}{W_0 - W_e} = 2\sum_{n=0}^{\infty} \frac{e^{-D_{eff}\beta_n^2 t}}{\beta_n^2 L^2} \quad (1)$$

$$\beta_n = (2n+1)\frac{\pi}{2L} \quad (2)$$

The equilibrium moisture values were estimated using the Modified Halsey equation (Eq. 3) obtained from literature (Soysal, 2001).

$$a_w = \exp[-\exp(2.97977 - 0.00258492T^{1.37743})W_e^{-1.44139}] \quad (3)$$

To estimate the equilibrium moisture content from equation 3 the relative humidity is needed. The relative humidity of the hot air was calculated from the hot air

97 temperature and the relative humidity and the temperature of the environment,
98 considering that the wet air behaves like a perfect gas.

99 The saturation pressure of water vapor in the wet air was estimated using an
100 equation obtained from literature (ASAE, 1999).

101 The experimental results were applied to fit the mathematical model obtaining the
102 value of the effective diffusivity (D_{eff}). Later, the dependence of the parameters on the
103 air temperature was analyzed applying the Arrhenius equation (Eq. 4)

$$D_{eff} = D_0 \exp\left(-\frac{E_a}{R(T + 273.16)}\right) \quad (4)$$

104

105 *2.3.2 Empirical models*

106 A search was performed to find mathematical models of the convective drying of
107 irregular shaped products, like thyme. Table 1 shows 7 widely used semi-theoretical
108 drying models (Doymaz, 2011), where ϖ is the dimensionless moisture content (Eq. 5)
109 and t is the time.

$$\omega(t) = \frac{W(t) - W_e}{W_0 - W_e} \quad (5)$$

110 The equilibrium moisture content values (W_e) were determined using equation 3,
111 from the experimental values of the hot air temperature, and the relative humidity and
112 temperature of the environment, considering that the wet air behaves like a perfect gas.

113 The experimental drying kinetics was used to fit mathematical models in order to
114 obtain the values of the model parameters. Subsequently, the dependence of the
115 parameters on the air temperature was analyzed, searching for polynomial relations in
116 order to obtain, in each case, a generic model that could predict the evolution of the
117 dimensionless moisture content in function of the time and temperature.

118

119 *2.3.3 Artificial Neural networks*

120 ANNs, a new generation of information processing paradigms designed to mimic
121 some of the behaviors of the human brain (Baş and Boyaci, 2007), has as main
122 advantage the fact that ANNs can simulate the nonlinear relationship between input and
123 output variables through a learning process, and generalize the knowledge among
124 homologous series without need for theoretical and empirical models.

125 Artificial neural networks were applied to predict the average moisture content
126 evolution and dimensionless moisture content: (i) one artificial neural network (ANN)
127 to predict the dimensionless moisture content evolution (ANN_r); (ii) a second ANN to
128 predict the average moisture content evolution (ANN_t).

129 The ANNs were developed considering the most common architecture, based on a
130 multilayer feed-forward structure with the back-propagation training algorithm used for
131 computing the ANN weights and biases. This architecture is the result of a "universal
132 approximation" (Hornik et al., 1989; Siegelman and Sontag, 1991) computing model
133 based on Kolmogorov's theorem (Kolmogorov, 1957) and the more comprehensive
134 observation done by R. Hecht-Nielsen (1990). There are two main ideas behind a
135 feedforward neural network: (i) the first idea is a full connection architecture, as the
136 outputs of neurons from the previous layer are connected with the corresponding inputs
137 of all neurons of the following layer; (ii) the second idea is a backpropagation learning
138 algorithm, when the errors of the neurons from the output layer are being sequentially
139 backpropagated through all the layers from the "right hand" side to the "left hand" side,
140 in order to calculate the errors of all other neurons. One more common property of a
141 major part of the feedforward networks is the use of sigmoid activation functions for its
142 neurons.

143 This is a type of network of supervised learning that is based on an algorithm of
144 descending gradients (Levenberg- Marquardt algorithm) (Levenberg, 1944; Marquardt,
145 1963), in order to minimize the error.
146 One of the problems that occur during neural network training is called overfitting.
147 The error on the training set is driven to a very small value, but when new data is
148 presented to the network, the error is large. The network has memorized the training
149 examples, but it has not learned to generalize to new situations (Lertworasirikul and
150 Saetan, 2010). To improve the generalization, the method called regularization was
151 applied, which updates the weight and bias values according to the Levenberg-
152 Marquardt optimization. It minimizes a combination of squared errors and weights, and
153 then determines the correct combination so as to produce a network that generalizes
154 well. The process is called Bayesian regularization (MacKay, 1992, Aggarwal et al.
155 2005).
156 There is no fixed rule for determining the required hidden layers and nodes. In
157 general, one hidden layer has been found to be adequate, and only in some cases, may a
158 slight advantage be gained by using two hidden layers (Lertworasirikul and Saetan,
159 2010). Therefore, although the number of hidden layers was fixed at one, this could be
160 increased if the fit wasn´t adequate, while the number of neurons in the hidden layer,
161 and transference functions between layers (tansig, logsig, purelin) were investigated.
162 To fit each ANN, a total of 273 data from 15 drying experiments were used. In the
163 ANN developed to predict the evolution of the dimensionless moisture content (ANN_r),
164 2 independent variables were considered: drying temperature (T) and time (t); as target
165 matrix, the dimensionless moisture content was applied. In the ANN developed to
166 predict the evolution of the average moisture content (ANN_t), 4 inputs were considered:
167 drying temperature (T), relative air humidity (h_r), initial sample moisture (W_0) and time

(t). With this ANN, the evolution of the average moisture content would be evaluated. The evolution of the value of the average moisture content depends both on the air conditions (T, h_r) and the initial moisture content (W_0), for which reason the variables h_r and W_0 were added as inputs. In this case, the average moisture content was considered as target matrix.

The proposed neural networks possessed a common structure: an input vector, with two components (T, t) (Figure 2a) or four components (T, t, h_r, W_0) (Figure 2b), one or two hidden layers with a number of neurons to be estimated, an output layer with 1 neuron, and 1 output (dimensionless moisture content or average moisture content). In the hidden layers the transfer function was studied, and the linear transfer function was applied in the output layer.

2.4 Statistical analysis

The average value of the percentage of the relative errors (ER) (Eq. 6) and the explained variance (VAR) statistics were used to evaluate the accuracy of fit (Bon et al., 2010). The average value of the relative errors is a measure of the random component in the estimation. VAR indicates the proportion of variance that is accounted for by the model.

$$ER = \frac{100}{N}\sum_{i=1}^{N}\frac{\left|Z_{exp_i} - Z_{cal_i}\right|}{Z_{exp_i}} \quad (6)$$

2.5 Computational tools

To fit the theoretical model, obtaining the value of the parameter D_{eff}, and to analyze the dependence of the D_{eff} fitting the Arrhenius equation, algorithms were

developed using Matlab® R2009a (The MathWorks, 2009) as the computational tool. The "nlinfit' function was applied to estimate the parameter values, by means of nonlinear regression, and the 'nlparci' function to estimate the confidence intervals for the parameters.

To fit the empirical models the Curve Fitting Toolbox of Matlab® R2009a was applied.

To develop the ANN, the Neural Network Toolbox™ of Matlab® R2009a was used. Using the Matlab languages, a function was developed to create, by applying the function "newff", and to train, by applying the function "train", a feed-forward backpropagation network. This function looked for the number of neurons in the hidden layers.

3. Results and discussion

3.1 Drying kinetic

Figure 3 shows the drying kinetics of thyme for different air temperatures; predictably, the drying rate increases as the air temperature rises. At the beginning of the drying process, when the moisture content of the product is high, the drying rate is relatively high; in the same way it can be observed that when the product moisture content decreases, the drying rate drops. As can be seen in Figure 3, at drying temperatures of 60 and 70°C, the drying time is reduced considerably by 76 and 85 %, compared to the drying total time at 40°C.

3.2 Theoretical model

213 The theoretical model was defined by considering several assumptions according
214 equation 1, as the external resistance to mass transfer was negligible. A way to assess
215 the relative importance of external resistance is by means of Eq. (7) (Mulet, 1994).

$$\frac{d\left[Ln(\omega)\right]}{dt} = \frac{(q + m\,\omega)^{0.5}}{\omega} \quad (7)$$

216 Plotting $\left(\omega\, d\left[Ln(\omega)\right]/dt\right)^2$ versus ϖ allows the prevailing resistance to be assessed.
217 When external resistance predominates, the plot is a straight line. Otherwise, it is a
218 parabola; as can be observed in Figure 4, the internal resistance governs mass transfer
219 during the drying process.

220 The estimated values of D_{eff} for all the drying conditions are presented in Table 2,
221 obtaining values between 3.68 10^{-5} and 2.12 10^{-4} s^{-1}. As expected, the values increased
222 greatly in line with the increase in drying temperature. The results show a good fit
223 between the experimental and estimated values (VAR ≥ 95.7%; ER ≤ 20.8%).

224 To fit the dependence of D_{eff} on the temperature (Equation 4) by means of a
225 nonlinear regression, the initial values of the parameters were estimated by fitting the
226 equation 4 linearized. Table 3 shows the parameter values obtained using the nonlinear
227 regression, obtaining activation energy with a value of 49.42 kJ/mol.

228

229 *3.3. Empirical models*

230 Dimensionless moisture content data versus drying time were fitted with the
231 different models listed in Table 1. Tables 4, 5, 6, and 7 show the results of non-linear
232 regression analysis performed to fit the empirical models for each drying temperature.
233 The results show a good fit between the experimental and estimated values of every
234 model (VAR ≥ 97.6%; ER ≤ 16.7 %). To analyze the dependence of the parameters of
235 the models with the temperature, polynomial equations were fitted, because previously

it was checked that the Arrhenius equation didn't estimate properly the relationship between the parameters and the temperature.

Table 8 shows the polynomial relations between parameters and temperature, and the statistical results of the fit of the polynomial equations. When these equations are considered in the corresponding model, generic models are obtained to be used in the temperature interval under consideration (40-70 ºC).

3.4. Artificial Neural Network

The number of hidden layers (between 1 and 3) and the number of neurons of each hidden layer (between 2 and 10), and the corresponding bias and weights numbers, was looked for, selecting the number hidden layers and the number of neurons for which the "best" values of the objective function applied in the training of the ANN was obtained. For that, the function created using the Matlab language was applied. Table 9 shows both the number of hidden layers, the number of neurons in the hidden layers and also the transfer function used in each ANN.

The correlation between the experimental and estimated values by neural networks can be seen in table 10.

3.5. Models comparison

Table 10 shows the statistical results of the application of the generic models, considering the experimental results for each temperature and considering all the experimental results. In every case, the designed neural networks show the best agreement for the drying curves of thyme, with VAR $\geq$ 99.3% and ER $\leq$ 2.9% for ANN_r, and with VAR$\geq$ 99.7% and ER $\leq$ 8.7% for ANN_t

4. Conclusions

Analyzing the influence of the temperature on the parameters of the models studied, generic models to estimate the evolution of dimensionless moisture content in function of the hot air temperature and drying time were obtained.

For the global application of the theoretical and empirical generic models analyzed, the Logarithmic model showed the best statistical results of the fit.

The fit of the theoretical diffusive model allowed estimating the effective diffusivity per unit area and the activation energy for the thyme variety used.

Both for individual cases (for each air hot temperature) to general cases (global application), the ANNs application showed the best statistical results of the fit. Therefore, the ANNs developed constitute an adequate model to predict the moisture content, representing the evolution of thyme drying better than either the theoretical model or the empirical models proposed. The models developed through ANNs would be of special interest in the formulation and optimization problems on line, and in the predictive control of process.

Acknowledgements

The authors of this work acknowledge the financial support from the "Ministerio de Educación y Ciencia" in Spain, CONSOLIDER INGENIO 2010 (CSD2007-00016).

References

Aggarwal, K. K., Singh, Y., Chandra, P., Puri, M. (2005). Bayesian Regularization in a Neural Network Model to Estimate Lines of Code Using Function Points. Journal of Computer Sciences, 1, (4), 505-509.

285 Akpinar, E.K. (2006). Mathematical modelling of thin layer drying process under open
286 sun of some aromatic plants. Journal of Food Engineering, 77, 864-870.
287 Akpinar, E. K., Bicer, Y., and Yildiz, C. (2003). Thin layer drying of red pepper.
288 Journal of Food Engineering, 59, 99-104.
289 AOAC. (1997). Official methods of analysis of AOAC International, 16th edn,
290 (Association of Official Analytical Chemist International AOAC, Gaithersburg,
291 USA).
292 Arslan, D. and Ozcan, M.M. (2008). Evaluation of drying methods with respect to
293 drying kinetics, mineral content and color characteristics of rosemary leaves.
294 Energy Conversion and Management, 49, 1258-1264.
295 ASAE. (1999). Psychrometric data, D271.2 DEC99. American Society of Agricultural
296 Engineers ASAE, USA.
297 Baş, D., and Boyaci, I.H. (2007). Modeling and optimization II: Comparison of
298 estimation capabilities of response surface methodology with artificial neural
299 networks in a biochemical reaction. Journal of Food Engineering, 78, 846-854.
300 Bon, J.,Váquiro, H., Benedito, J. and Telis-Romero, J. (2010). Thermophysical
301 properties of mango pulp (Mangifera indica L. cv. Tommy Atkins). Journal of
302 Food Engineering, 97, 563-568.
303 Chegini, G.R. (2008). Prediction of process and product parameters in an orange juice
304 spray drying using artificial neural network. Journal of Food Engineering, 84,
305 534.
306 Clemente, G., Bon, J., Sanjuán, N., Mulet, A. (2011). Drying modelling of defrosted
307 pork meat under forced convection conditions. Meat Science, 88, 374-378.

Doymaz, I. (2011). Drying of Thyme (Thymus Vulgaris L.) and selection of a suitable thin-layer drying model. Journal of Food Processing and Preservation. doi: 10.1111/j.1745-4549.2010.00488.x.

Doymaz, I. (2009). Thin-layer drying of spinach leaves in a convective dryer. Journal of Food Process Engineering, 32, 112-125.

Erenturk S. and Erenturk K., (2007). Comparison of genetic algorithm and neural network approaches for the drying process of carrot. Journal of Food Process Engineering, 78(3), 905-912.

Ghodake, H.M., Goswami, T.K. and Chakraverty, A. (2006).Mathematical modeling of withering characteristics of tea leaves. Drying Technology, 24, 159-164.

Hecht-Nielsen, R. (1990) Neurocomputing. Addison Wesley, New York.

Hornik, K., Stinchcombe, M.,White, H. (1989). Multilayer feedforward neural networks are universal approximators. Neural Netw 2:259–366

Kolmogorov, A.N. (1957). On the representation of continuous functions of many variables by superposition of continuous functions and addition (in Russian). The Reports of theAcademy of Sciences of the USSR. Doklady Akademii Nauk SSSR 114:953–956.

Lee, J.H. and Kim, H.J. (2008). Drying kinetics of onion slices in a hot-air dryer. Journal of Food Science & Nutrition, 13, 225-230.

Lertworasirikul, S. and Saetan, S., (2010). Artificial neural network modeling of mass transfer during osmotic dehydration of kaffir lime peel. Journal of Food Engineering, 98(2), 214-223.

Maskan, M. (2001). Kinetics of color change of kiwifruits during hot air and microwave drying. Journal of Food Engineering, 48, 169-175.

MacKay, D.J.C. (1992). A Practical Bayesian Framework for Backpropagation Networks. Neural Computation, 4(3), 448-472.

Mcminn, W.A.M. (2006). Thin-layermodeling of the convective, microwave, microwave-convective and microwave-vacuum drying of lactose powder. Journal of Food Engeneering, 72, 113-123.

Mulet, A. (1994). Drying modelling and water diffusivity in carrots and potatoes. Journal of Food Engineering, 22, 329-348.

Ozdemir, M. and Devres, Y.O. (1999). The thin layer drying characteristics of hazelnuts during roasting. Journal of Food Engineering, 42, 225-233.

Sablani, S.S. and Rahman, M.S. (2003). Using neural networks to predict thermal conductivity of food as a function of moisture content, temperature and apparent porosity. Food Research International, 36, 617-623.

Sanjuán, N., Lozano, M., Garcia-Pascual, P. and Mulet, A. (2003). Dehydration kinetics of red pepper (Capsicum annuum L var Jaranda). Journal of the Science of Food and Agriculture, 83(7), 697-701.

Shati, A.A. and Elsaid, F.G. (2009). Effects of water extracts of thyme (Thymus vulgaris) and ginger (Zingiber officinale Roscoe) on alcohol abuse. Food Chemical and Toxicology, 47, 1945-1949.

Siegelman, H. and Sontag, E. (1991). Neural nets are universal computing devices. Research Report SYCON-91–08. Rutgers Center for Systems and Control. Rutgers University

Soysal Y. and Oztekin S. (2001). Comparison of seven equilibrium moisture content equations for some medicinal and Aromatic. Journal of Agricultural Engineering Research, 78(1), 57-63.

The MathWorks. (2009). MATLAB user's guide. The MathWorks Inc., SouthNatick, MA, USA.

Zhou, W. and Therdthai, N. (2010). Special topics in Food Engineering: Artificial neural networks in food processing,, In D. Sun (Ed), Mathematical Modeling of Food Processing (pp. 901-920). Boca Raton: CRC Press.

NOMENCLATURE

a, a_l, a_{Te}, a_{Pb}	Dimensionless parameters of empirical models
ANN	Artificial neural network
ANN_r	ANN developed to predict the evolution of the dimensionless moisture content
ANN_t	ANN developed to predict evolution of the average moisture content
a_w	Parameters of empirical model (s^{-1})
a_w	Water activity
b, b_H, b_L, b_{Te}, b_{Pb}	Parameters of empirical models (s^{-1})
b_P	Parameter of empirical model (s^{-c})
b_W	Parameter of empirical model (s^{-2})
c, c_L,	Dimensionless parameters of empirical models
c_{Pb}	Parameter of empirical model (s^{-2})
D_{eff}	Effective diffusivity (s^{-1})
D_o	Parameter of the Arrhenius equation (s^{-1})
E_a	Activation energy (kJ/mol)
ER	Average value of the relative errors (%)
h_r	Relative humidity
L	Semi-thickness of the bed (m)

m	Parameter of equation 11
N	Number of observations
q	Parameter of equation 11
R	Constant of perfect gas (kJ/mol K)
T	Air temperature (ºC)
t	Drying time (s, min)
VAR	Explained variance (%)
W	Average moisture content, in dry basis (kg /kg)
W_0	Initial moisture content, in dry basis (kg /kg)
W_e	Equilibrium moisture content, in dry basis (kg/kg)
Z_{cal}	Calculated value of a property
Z_{exp}	Experimental value of a property
ϖ	Dimensionless moisture content

363

364

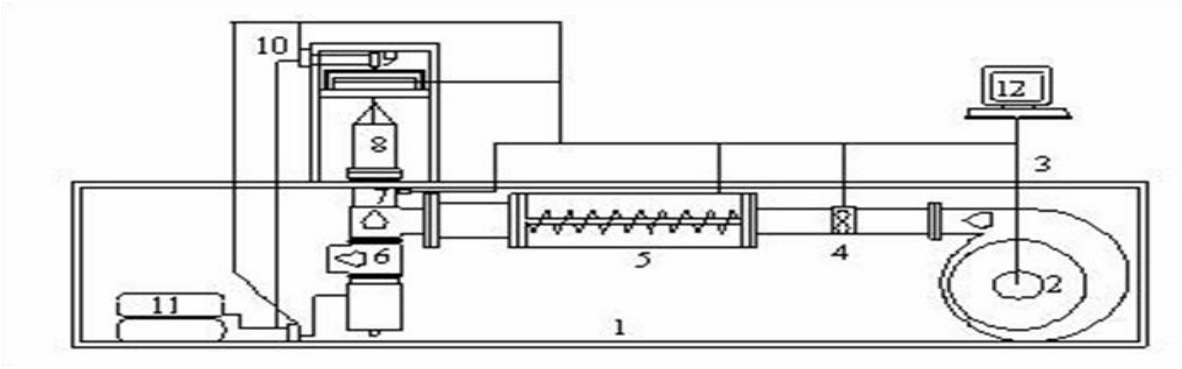

Figure 1. Schema of an automatic convective drier on a laboratory scale. 1) Support; 2) Fan; 3) Flow control; 4) Anemometer; 5) Electrical resistance; 6) Pneumatic valve; 7)Temperature sensor; 8) Drying chamber; 9) Balance; 10) Elevator; 11) Air compressor; 12) Control and data acquisition

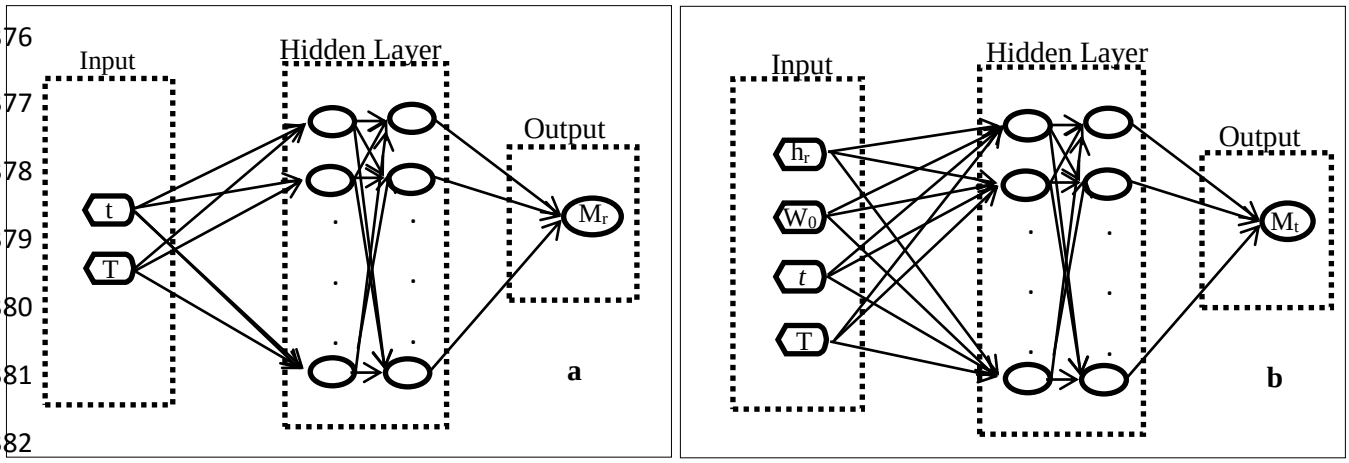

Figure 2. Neural network schemes. a) Inputs vector with two components; b) Inputs vector with four components.

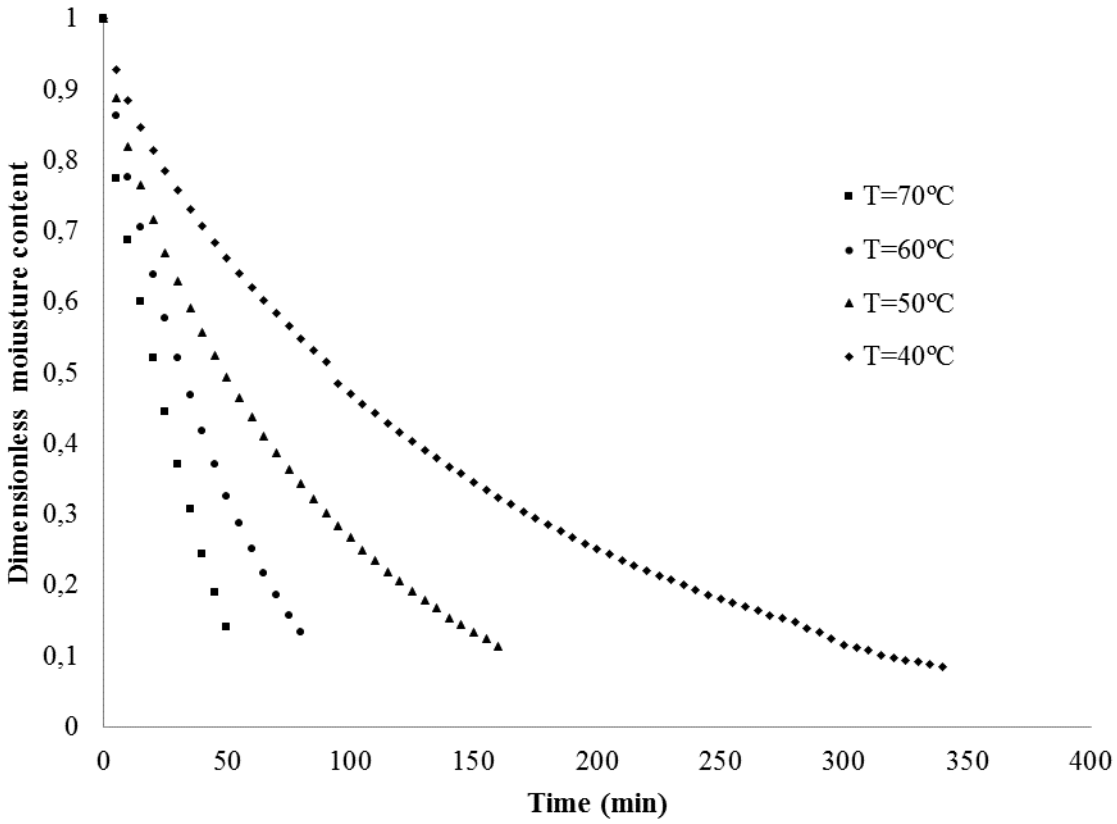

386

387 **Figure 3.** Thyme drying at different air temperatures

388

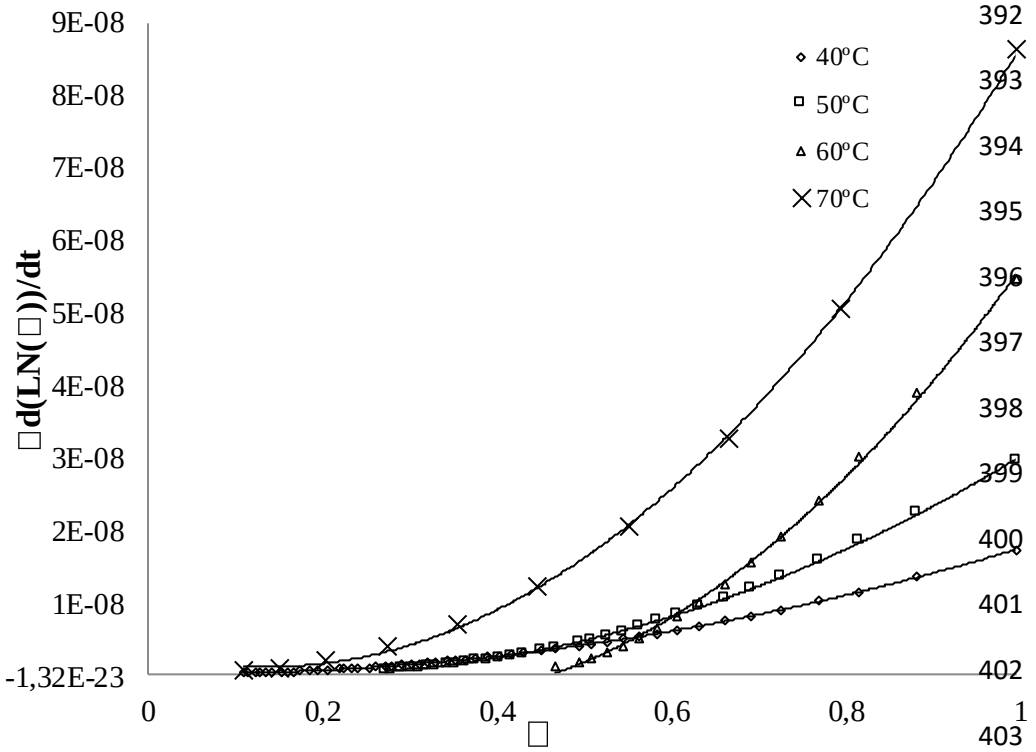

Figure 4. Influence of external resistance on drying kinetics of thyme

410 **Table 1.** Empirical models selected

Model name	**Model**
Newton	$M_r = \exp(-b\ t)$
Henderson and Pabis	$M_r = a \exp(-b_H\ t)$
Page	$M_r = \exp(-b_P\ t^c)$
Logarithmic	$M_r = a_L \exp(-b_L\ t) + c_L$
Two-term exponential	$M_r = a_{Te} \exp(-b_{Te}\ t) + (1 - a_{Te}) \exp(-b_{Te}\ a_{Te}\ t)$
Wang and Singh	$M_r = 1 + a_W\ t + b_W\ t^2$
Parabolic	$M_r = a_{Pb} + b_{Pb}\ t + c_{Pb}\ t^2$

411

412 **Table 2**. Values of effective diffusivity per unit area at different hot air temperatures (D_{eff}
413 ± standard deviation)·10^{-9} (s^{-1}). 95% confidence intervals

Temperature (°C)	**D_{eff} (s^{-1})**	**Confidence bounds**		**ER (%)**	**VAR (%)**
		Lower	**higher**		
40	7.7± 1.14	7.4	8.0	20.8	95.7
50	15.2 ± 1.17	14.7	15.7	11.0	98.5
60	27.6 ± 2.49	25.7	29.6	17.4	97.5
70	44.5 ± 1.41	44.4	48.6	18.4	98.3

414 Relative error (ER) considering the dimensionless moisture content

415

416 **Table 3**. Results of the fit of the Arrhenius equation. 95% confidence intervals

Parameter	**Value**	**Confidence bounds**		**ER (%)**	**VAR (%)**
		Lower	**higher**		
D_0 (s^{-1})	7855	-1879	34500	3.6	99.8
E_a (kJ/mol)	49.42	40.05	58.80		

417

Table 4. Results of the fitting of empirical models using experimental results obtained by air drying at 40ºC.

Model	Models parameters						VAR (%)	ER (%)
Newton	b	$1.4\ 10^{-4} \pm 2.6\ 10^{-5}$					99.2	7.2
Henderson and Pabis	a	0.913 ± 0.0	b_H	$1.4\ 10^{-4} \pm 0.0$			99.4	16.7
Page	b_P	$4.0\ 10^{-4} \pm 2.1\ 10^{-5}$	c	0.89675 ± 0.05			99.8	3.5
Logarithmic	a_L	0.8807 ± 0.0	b_L	$1.7\ 10^{-4} \pm 0.0$	c_L	0.05746 ± 0.0	99.7	12.2
Two-term exponential	a_{Te}	0.28265 ± 0.02	b_{Te}	$2.1\ 10^{-4} \pm 2.1\ 10^{-5}$			99.6	4.3
Wang and Singh	a_W	$-1.1\ 10^{-4} \pm 1.6\ 10^{-5}$	b_W	$3.74\ 10^{-9} \pm 1.1\ 10^{-9}$			99.9	12.7
Parabolic	a_{Pb}	0.8906 ± 0.076	b_{Pb}	$-9.0\ 10^{-5} \pm 1.2\ 10^{-5}$	c_{Pb}	$2.7\ 10^{-9} \pm 7.6\ 10^{-10}$	99.2	5.9

Table 5. Results of the fitting of empirical models using experimental results obtained by air drying at 50ºC.

Model	Models parameters						VAR (%)	ER (%)
Newton	b	$2.3\ 10^{-4} \pm 1.4\ 10^{-5}$					99.2	8.3
Henderson and Pabis	a	0.9668 ± 0.02	b_H	$2.3\ 10^{-4} \pm 3.0\ 10^{-5}$			99.7	3.7
Page	b_P	$2.8\ 10^{-4} \pm 1.0\ 10^{-4}$	c	0.98983 ± 0.04			99.8	4.5
Logarithmic	a_L	1.10853 ± 0.23	b_L	$2.3\ 10^{-4} \pm 4.1\ 10^{-6}$	c_L	$0.01858 \pm 0.1\ 10^{-3}$	99.7	7.1
Two-term exponential	a_{Te}	1.01350 ± 0.02	b_{Te}	$2.5\ 10^{-4} \pm 2.1\ 10^{-5}$			99.1	4.2
Wang and Singh	a_W	$-1.0\ 10^{-4} \pm 1.9\ 10^{-5}$	b_W	$1.36\ 10^{-8} \pm 2.5\ 10^{-9}$			99.9	10.0
Parabolic	a_{Pb}	0.92746 ± 0.013	b_{Pb}	$-1.7\ 10^{-4} \pm 2.0\ 10^{-5}$	c_{Pb}	$9.3\ 10^{-9} \pm 1.1\ 10^{-9}$	99.2	5.1

Table 6 Results of the fitting of empirical models using experimental results obtained by air drying at 60ºC.

Model	Models parameters						VAR (%)	ER (%)
Newton	b	$3.9\ 10^{-4} \pm 1.4\ 10^{-5}$					97.5	8.7
Henderson and Pabis	a	1.0131 ± 0.02	b_H	$3.9\ 10^{-4} \pm 2.8\ 10^{-5}$			98.1	9.0
Page	b_P	$1.8\ 10^{-4} \pm 3.2\ 10^{-5}$	c	1.094 ± 0.15			99.8	8.2
Logarithmic	a_L	1.133 ± 0.66	b_L	$2.3\ 10^{-4} \pm 8.2\ 10^{-6}$	c_L	$-0.15505 \pm 6.63\ 10^{-2}$	99.2	3.1
Two-term exponential	a_{Te}	1.568 ± 0.13	b_{Te}	$4.5\ 10^{-4} \pm 2.6\ 10^{-4}$			99.2	4.1
Wang and Singh	a_W	$-3.1\ 10^{-4} \pm 1.2\ 10^{-5}$	b_W	$2.48\ 10^{-8} \pm 6.1\ 10^{-9}$			98.8	4.3
Parabolic	a_{Pb}	$0.9717 \pm 8.0\ 10^{-3}$	b_{Pb}	$-2.8\ 10^{-4} \pm 7.3\ 10^{-6}$	c_{Pb}	$2.1\ 10^{-9} \pm 5.6\ 10^{-10}$	99.5	3.4

Table 7. Results of the fitting of empirical models using experimental results obtained by air drying at 70ºC.

Model	Models parameters						VAR (%)	ER (%)
Newton	b	$5.4\ 10^{-4} \pm 5.0\ 10^{-5}$					99.2	11.9
Henderson and Pabis	a	1.02936 ± 0.04	b_H	$5.5\ 10^{-4} \pm 4.1\ 10^{-5}$			99.4	10.8
Page	b_P	$1.2\ 10^{-4} \pm 2.1\ 10^{-5}$	c	1.26433 ± 0.16			99.8	9.1
Logarithmic	a_L	1.25743 ± 0.28	b_L	$4.0\ 10^{-4} \pm 1.2\ 10^{-4}$	c_L	-0.27942 ± 0.0213	99.7	6.2
Two-term exponential	a_{Te}	1.01350 ± 0.16	b_{Te}	$2.5\ 10^{-4} \pm 2.4\ 10^{-4}$			99.6	5.8
Wang and Singh	a_W	$-3.8\ 10^{-4} \pm 4.6\ 10^{-5}$	b_W	$3.3\ 10^{-8} \pm 1.7\ 10^{-8}$			99.9	3.3
Parabolic	a_{Pb}	0.98566 ± 0.02	b_{Pb}	$-4.0\ 10^{-4} \pm 2.5\ 10^{-5}$	c_{Pb}	$4.1\ 10^{-9} \pm 3.1\ 10^{-10}$	99.2	2.6

Table 8. Empirical relations between parameters and temperature, and statistical results.

			VAR (%)	ER (%)
Newton	b	$1.338\ 10^{-5}T - 0.00041$	99.3	6.5
Henderson and Pabis	a	0.991 ± 0.051		
	b_H	$1.413\ 10^{-5}T - 4.432\ 10^{-4}$	99.3	7.1
Page	b_P	$-8.531\ 10^{-6}\ T + 7.196\ 10^{-4}$	97.5	15.8
	c	$1.134\ 10^{-2}\ T + 4.337\ 10^{-1}$	98.3	1.7
Logarithmic	a_L	$1.394\ 10^{-2}\ T + 2.880\ 10^{-1}$	94.6	4.1
	b_L	$6.813\ 10^{-6}T - 1.060\ 10^{-4}$	96.7	4.2
	c_L	$-2.484\ 10^{-4}\ T^2 + 1.534\ 10^{-2}\ T - 1.517\ 10^{-1}$	98.6	13.1
Two term exponential	a_{Te}	$-1.148\ 10^{-3}\ T^2 + 1.757\ 10^{-1}\ T - 4.9017$	99.3	2.9
	b_{Te}	$3.163\ 10^{-7}\ T^2 - 1.965\ 10^{-5}\ T + 4.763\ 10^{-4}$	99.3	7.2
Wang and Singh	a_W	$-9.042\ 10^{-6}\ T + 2.494\ 10^{-4}$	99.3	3.6
	b_W	$1.148\ 10^{-9}\ T - 4.357\ 10^{-8}$	97.8	13.2
Parabolic	a_{Pb}	$-4.619\ 10^{-5}\ T^2 + 8.419\ 10^{-3}\ T + 6.265\ 10^{-1}$	99.1	4.1
	b_{Pb}	$-1.060\ 10^{-5}\ T + 3.445\ 10^{-4}$	99.6	5.7
	c_{Pb}	$2.826\ 10^{-11}\ T^2 - 1.874\ 10^{-9}\ T + 3.232\ 10^{-8}$	99.8	3.6

Table 9. Number of hidden layers and number of neurons in the hidden layers

	Transfers function	Number of hidden layers	Number of neurons	VAR (%)	ER (%)
ANN_r	Tansig	1	10	97.8	10.1
	Logsig	1	10	96.9	9.2
	Purelin	1	10	78.9	24.3
ANN_t	Tansig	1	10	98.7	8.9
	Logsig	1	10	98.8	7.6
	Purelin	1	10	79.9	18.9
ANN_r	Tansig	2	6/4	99.7	3.7
	Logsig	2	5/5	98.7	2.8
	Purelin	2	4/4	78.9	18.9
ANN_t	Tansig	2	5/5	99.9	1.6
	Logsig	2	5/6	99.9	3.4
	Purelin	2	4/2	84.4	24.3

Table 10. Statistical results of the fit (for all experimental results) and of the application (40, 50, 60 and 70 ºC) of the generic models.

		40°C		50°C		60°C		70°C		For all experimental results	
		VAR (%)	ER (%)	VAR (%)	ER (%)	VAR (%)	ER (%)	VAR (%)	ER (%)	VAR (%)	ER (%)
Theoretical model		99.5	5.6	99.7	5.5	98.4	3.7	97.1	19.5	93.4	17.8
Empirical models	**Newton**	99.3	14.7	99.6	12.7	99.2	8.5	98.6	14.0	97.1	13.0
	Henderson and Pabis	99.3	14.4	99.5	13.8	99.2	8.7	98.4	12.4	96.9	13.2
	Page	99.5	13.3	99.1	23.5	98.7	23.2	98.3	21.1	96.7	18.5
	Logarithmic	99.1	12.2	99.7	8.9	99.6	8.2	99.4	13.9	97.5	10.4
	Two-term exponential	99.1	68.6	99.3	19.0	99.5	12.7	99.3	20.5	87.3	39.6
	Wang and Singh	93.4	50.8	91.4	56.2	99.6	8.1	99.4	45.1	92.1	40.4
	Parabolic	97.2	52.2	99.2	31.2	99.5	13.7	99.4	8.7	89.6	35.5
ANN Models	**ANN_r**	99.9	0.6	99.8	1.4	99.7	1.4	99.3	2.9	99.7	3.7
	ANN_t	99.9	0.8	99.9	0.7	99.9	3.3	99.7	8.7	99.9	1.6

Relative error (ER) was calculated considering the dimensionless moisture content, except for ANN_t, where the ER is calculated considering the average moisture content, in d.b.